

# Asymptotic Modal Analysis of a Rectangular Acoustic Cavity Excited by Wall Vibration

Linda F. Peretti\* and Earl H. Dowell†  
Duke University, Durham, North Carolina 27706

Asymptotic modal analysis, a method that has recently been developed for structural dynamical systems, has been applied to a rectangular acoustic cavity. The cavity had a flexible vibrating portion on one wall, and the other five walls were rigid. Banded white noise was transmitted through the flexible portion (plate) only. Both the location along the wall and the size of the plate were varied. The mean square pressure levels of the cavity interior were computed as a ratio of the result obtained from classical modal analysis to that obtained from asymptotic modal analysis for the various plate configurations. In general, this ratio converged to 1.0 as the number of responding modes increased. Intensification effects were found due to both the excitation location and the response location. The asymptotic modal analysis method was both efficient and accurate in solving the given problem. The method has advantages over the traditional methods that are used for solving dynamics problems with a large number of responding modes.

## Nomenclature

$A$	= area
$c$	= speed of sound
$F$	= cavity acoustic modal function
$L$	= cavity dimension
$M$	= generalized mass
$p$	= pressure
$r$	= modal index
$V$	= volume
$w$	= displacement
$X, Y, Z$	= acoustic modal function component dependent on $x, y, z$
$x, y, z$	= spatial position coordinates
$\Delta N$	= number of acoustic modes
$\zeta$	= damping ratio
$\rho$	= density
$\Phi$	= power spectrum
$\omega$	= frequency
$\langle \rangle$	= spatially averaged quantity
$\cdot$	= time derivative
$-$	= rms

## Subscripts

$c$	= center frequency
$f$	= flexible
$o$	= reference value
$r$	= acoustic modal index
$w$	= pertaining to the flexible wall

## Superscripts

$A$	= acoustic
-----	------------

## Introduction

**C**OUPLED structural-acoustic systems are encountered often in aeronautical applications. Accurate, efficient means of analysis are central to the design of structures with the desired sound transmittal properties. Two analytical meth-

ods that are commonly used to solve such coupled systems are classical modal analysis (CMA) and statistical energy analysis (SEA). Recently, Dowell<sup>1</sup> and others<sup>2-4</sup> have developed an additional method, asymptotic modal analysis (AMA), which can also be applied to structural-acoustic systems.

AMA incorporates the advantages of the other two methods. Providing there are a large number of modes, the CMA result and the AMA result are nearly identical. Since it does not need to take the individual modal contributions into account, the computation cost of AMA is significantly less. An added advantage of AMA is that the degree of generality in the final result can be controlled by adjusting the types of assumptions and/or simplifications made in the derivation. This feature allows the use of AMA to obtain results identical to SEA or, for example, to relax the averaging simplifications and obtain local response results of which SEA is not capable.

To explore the capabilities of AMA, the interior sound field of a rectangular acoustic cavity was analyzed mathematically. The ratio of response predicted by CMA to that predicted by AMA was calculated either as a spatial average or at particular locations inside the cavity. Five of the cavity walls were rigid. A random white noise sound field passed through a portion of the sixth wall into the interior of the cavity. The flexible vibrating portion was varied in size and location, and the resulting sound pressure levels (mean square pressures) in the interior were calculated using AMA and CMA and then compared.

Local response peaks, or intensification zones, were observed at boundary points, while the response in the interior region was nearly uniform. Sound pressure levels were affected by the location and size of the flexible vibrating portion of the wall (sound source). In general, sound pressure levels increased by a factor of 4 when a point was placed in the corner. Also, for small sound sources (smaller than an acoustic wavelength) that are placed in the center of the wall, lines of symmetry become regions of increased sound pressure level.

## Background

SEA has been used to study the high-frequency interaction between large, complex, multimodal structures and acoustic spaces. The basic assumption underlying SEA is that the dynamic parameters in the system behave stochastically. SEA relates the power of the applied forces to the energy of the coupled systems and produces a set of linear equations that can be solved for the energy in each system. The energy in the system is the variable of primary interest, and other variables such as displacement, pressure, etc., are found from the energy of vibration. SEA has its advantages, as well as its limitations.

Received Jan. 2, 1991; revision received June 18, 1991; accepted for publication June 26, 1991. Copyright © 1991 by the American Institute of Aeronautics and Astronautics, Inc. All rights reserved.

\*Research Assistant Professor, Department of Mechanical Engineering and Materials Science, School of Engineering.

†Professor and Dean, Department of Mechanical Engineering and Materials Science, School of Engineering. Fellow AIAA.

The main advantage of SEA is its ability to describe the sound field without having to consider the individual modes. Statistical energy analysis also allows for a much simpler description of the system, requiring only parameters such as modal density, average modal damping, and certain averages of modal impedance to sound sources. The most significant disadvantage of using a statistical approach is that it is only valid for systems whose order is sufficiently high that the stochastic assumptions apply. Certain frequency bandwidths may not contain enough modes to allow the underlying assumptions to hold, rendering the SEA result unreliable. In addition, the local response information is lost in the SEA treatment. The text by Lyon<sup>5</sup> is the standard reference on SEA.

Dowell<sup>1</sup> has shown that results identical to those calculated using SEA can be obtained by studying the asymptotic behavior of CMA for a general, linear (structural) system; this asymptotic approach is AMA. AMA is basically a modal sum method. It possesses all of the computational advantages of SEA, in that the individual modal characteristics do not play a role in the asymptotic analysis. Additionally, AMA has advantages that SEA does not. Since AMA results can be derived systematically from CMA, AMA allows an assessment of the assumptions and consequent simplifications that are made to obtain such results. Also, by using a combination of CMA and AMA, results can be obtained for all frequency bandwidths of interest, not just those with a sufficiently high number of modes. And finally, AMA has predicted local response peaks, or intensification zones, results unobtainable using SEA.<sup>3,4</sup>

Previous work for structural systems has shown that the asymptotic behavior of AMA depends on the number of modes in a frequency interval of interest and the location of point forces. In the limit of an infinite number of modes, all points on the structure have the same response except for some special areas. The exceptional areas (intensification zones) are near the points of excitation and near the structural system boundary.<sup>3,4</sup> Numerical examples were presented for a beam in Ref. 2. Crandall,<sup>6</sup> Itao and Crandall,<sup>7</sup> and Crandall and Kulvets<sup>8</sup> experimentally found intensification zones in their work with structures. The response of a rectangular plate under a point random force was investigated by Kubota and Dowell,<sup>3</sup> and AMA calculations were found to agree closely with experimental measurements.

Work has also been done using AMA for structural-acoustic systems. Kubota et al.<sup>4</sup> examined a rectangular acoustic cavity with one vibrating wall (the other five rigid). They assumed that the vibrating wall had an infinite number of structural modes responding and that the entire wall was oscillating. The results obtained from the numerical study indicated that the spatially averaged CMA response approaches the AMA response as the number of modes increases. The local asymptotic response revealed an almost uniform distribution in the cavity interior, with peaks at the boundaries (sides, edges, and corners) of the cavity. Here, an AMA method is presented and new results obtained for structural-acoustic systems where only a portion of the wall vibrates rather than the entire wall, and both the size and location of the oscillating portion are varied.

### Theory

Most coupled structural acoustic problems are modeled using either CMA, summing for the response of each mode, or SEA, which combines the predicted energies of the subsystems and coupling loss factors to obtain a final result. In this work, a comparison is made between the CMA result and the AMA result as the number of acoustic modes and the number of structural modes approaches infinity. Note that the spatially averaged AMA result is identical to the SEA result.

In order to calculate the response of the interior acoustic cavity to the transmission of noise through a structural wall on its boundary, both the structural modes of the wall and the

acoustic modes of the interior must be considered. As derived in Ref. 4, the CMA result for the mean square pressure at a point  $(x, y, z)$  in a structural-acoustic enclosure is

$$\frac{\bar{p}^{-2}}{(\rho_o c_o^2)^2} \equiv \frac{\pi}{4} \frac{A_f}{V^2} \Phi_w(\omega_c) \sum_r \frac{F_r^2(x, y, z)}{(M_r^A)^2 (\omega_r^A)^3 \zeta_r^A} \times \iint_{A_f} F_r^2(x, y, z_o) dx dy \quad (1)$$

Implicit in this result are the following assumptions: the number of structural modes within the frequency band of interest is large (i.e., approaches infinity), and the power spectrum of the wall response is slowly varying with respect to frequency relative to the rapidly varying acoustic modal transfer function. As a result of these assumptions, the modal dynamics of the structure are effectively removed from the problem. In other words, the structural system is described in the AMA limit, whereas the acoustic system is taken in the CMA limit. Further, it is assumed that the modal damping ratio is small ( $\ll 1$ ), which removes the coupling between acoustic modes (see Ref. 9 for justification).

To obtain the AMA result for the acoustic cavity, further assume that the acoustic generalized mass squared  $(M_r^A)^2$ , the frequency of the acoustic mode cubed  $(\omega_r^A)^3$ , and the acoustic damping  $(\zeta_r^A)$  do not vary rapidly with respect to modal number  $r$  and can therefore be replaced by their values at the center frequency,  $(M_c^A)^2$ ,  $(\omega_c^A)^3$ , and  $(\zeta_c^A)$ . Moreover, the expression

$$\sum_r F_r^2(x, y, z) \iint_{A_f} F_r^2(x, y, z_o) dx dy$$

is approximately equal to the average of  $F_r^2(x, y, z)$  times

$$\sum_r \iint_{A_f} F_r^2(x, y, z_o) dx dy \quad \text{as } r \rightarrow \infty$$

(i.e., a large number of acoustic modes). The previous expression can be further simplified by

$$\sum_r \iint_{A_f} F_r^2(x, y, z_o) dx dy = \sum_r A_f \langle X_r^2 \rangle_{A_f} \langle Y_r^2 \rangle_{A_f} \langle Z_r^2(z_o) \rangle_{A_f}$$

where the right-hand side reduces to

$$A_f \Delta N^A \frac{\langle F_c^2 \rangle}{\langle Z_c^2 \rangle}$$

where  $\langle Z_c^2 \rangle = \langle F_c^2 \rangle / \langle F_c^2 \rangle_{A_f}$ . Here,  $\langle F_c^2 \rangle$  is a volume average, and  $\langle F_c^2 \rangle_{A_f}$  is an average over the vibrating structural wall area. Then,

$$\frac{\bar{p}^{-2}}{(\rho_o c_o^2)^2} \equiv \frac{\pi \Phi_w(\omega_c) A_f^2 \langle F_c^2 \rangle \sum_r F_r^2(x, y, z)}{4 V^2 (M_c^A)^2 (\omega_c^A)^3 \zeta_c^A \langle Z_c^2 \rangle} \quad (2)$$

This result is the AMA representation for the acoustic cavity, which assumes that there are both a large number of acoustic modes and a large number of structural modes. It is valid at any point  $x, y, z$  inside the acoustic cavity and is not a spatial average. The spatial average of Eq. (2) is

$$\frac{\langle \bar{p}^2 \rangle}{(\rho_o c_o^2)^2} \equiv \frac{\pi}{4} \left( \frac{A_f}{V} \right)^2 \frac{\Delta N}{\Delta \omega^A} \frac{\langle \bar{\omega}^2 \rangle_{\Delta \omega}}{(\omega_c^A)^3 \zeta_c^A \langle Z_c^2 \rangle} \quad (3)$$

This expression is referred to as the spatially averaged AMA result ( $\langle \text{AMA} \rangle$ ) and is used as the denominator throughout the analysis.

The effect of the source position is included in the term  $\langle Z_c^2 \rangle$ , which is a ratio of the spatially averaged modal functions over the volume to that over the flexible wall area. Except for this term, the expression in Eq. (3) is independent of the

cavity geometry. The  $\langle Z_c^2 \rangle$  ratio will always be of order 1. Specifically, for a rectangular geometry when the flexible portion is well removed from a corner or an edge, or for a cylindrical cavity with a vibrating portion on one of the ends (but away from the edge),  $\langle Z_c^2 \rangle = 1/2$ . The usual AMA result assumes this value of  $\langle Z_c^2 \rangle$ ; however, the cases where the flexible portion is placed at a corner or an edge are easily accounted for in the  $\langle Z_c^2 \rangle$  term and result in an additional multiplicative factor of  $1/4$  or  $1/2$ , respectively.

In order to separate the effects of the response position inside the cavity from the position of the flexible portion  $A_f$  of the wall (source position), two ratios were used,  $\langle CMA \rangle / \langle AMA \rangle$  and  $CMA_{\text{local}} / \langle AMA \rangle$ . Several combinations of CMA and AMA, spatially averaged and local results, were possible. The motivation for the choice of these particular ratios is presented in the Discussion section of this paper. The first ratio, comparing the spatial averages computed by the two methods, is used to demonstrate the convergence of the CMA results toward AMA as a function of frequency. The spatially averaged results are also used to demonstrate the overall effect of excitation position on sound pressure level. The second ratio is used to study local behavior at particular points inside the acoustic cavity. This ratio is therefore used to demonstrate the effect of response position independent of source position, as well as the combined effects of source position and local response position.

The ratio of the spatial average of CMA to the spatial average of AMA is

$$\frac{\langle CMA \rangle}{\langle AMA \rangle} = \sum_r \frac{\langle F_r^2(x, y, z) \rangle \iint_{A_f} F_r^2(x, y, z_o) dx dy (\omega_c^A)^3 \langle Z_c^2 \rangle}{(M_r^A)^2 (\omega_r^A)^3 \Delta N^A A_f} \quad (4)$$

This expression is derived in Ref. 4 and can be obtained from Eqs. (1) and (3). Equation (4) was used to assess the effect of excitation size and location due to area change and position of the vibrating portion of the wall.

The separate effect of response position was studied by taking the ratio of the local mean square pressure predicted with CMA to the spatially averaged mean square pressure predicted by AMA:

$$\frac{\langle CMA \rangle}{\langle AMA \rangle} = \frac{(\omega_c^A)^3 \langle Z_c^2 \rangle}{\Delta N^A A_f} \sum_r \frac{F_r^2(x, y, z) \iint_{A_f} F_r^2(x, y, z_o) dx dy}{(M_r^A)^2 (\omega_r^A)^3} \quad (5)$$

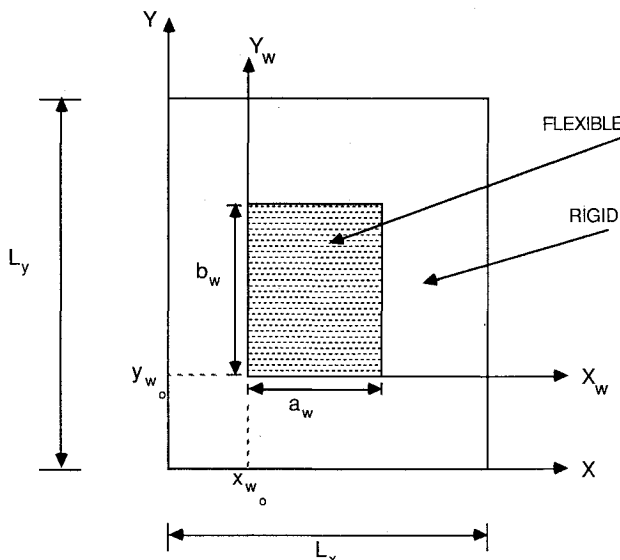


Fig. 1 Flexible vibrating portion of one wall of the cavity.

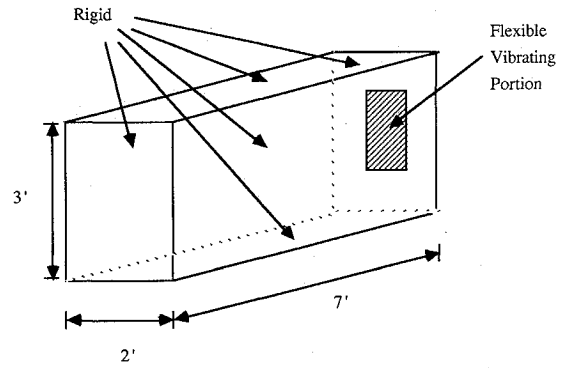


Fig. 2 Rectangular acoustic cavity with a portion of one wall flexible and vibrating.

Equations (1-5) hold for any cavity geometry.

### Rectangular Cavity

Dowell et al.<sup>10</sup> have shown that the acoustic pressure for a rectangular cavity with a flexible wall (all others rigid) can be described by the well-known rigid wall expansion or hard box modes for the structure:

$$F_r(x, y, z) = \cos\left(\frac{r_x \pi x}{L_x}\right) \cos\left(\frac{r_y \pi y}{L_y}\right) \cos\left(\frac{r_z \pi z}{L_z}\right)$$

In this analysis, the flexible portion of the structural wall is allowed to vary both in size and position. Therefore, the integral

$$\iint_{A_f} F_r^2(x, y, z_o) dx dy$$

in Eqs. (4) and (5) becomes

$$\int_0^{a_w} \int_0^{b_w} \cos^2\left[\frac{r_x \pi (x_{w_o} + x_w)}{L_x}\right] \cos^2\left[\frac{r_y \pi (y_{w_o} + y_w)}{L_y}\right] \times \cos^2\left(\frac{r_z \pi z_o}{L_z}\right) dx_w dy_w$$

where  $r_x$ ,  $r_y$ , and  $r_z$  are modal indices, and  $x_{w_o}$ ,  $y_{w_o}$ ,  $x_w$ ,  $y_w$ ,  $L_x$ , and  $L_y$  are defined in Fig. 1. This integral can then be evaluated analytically in terms of the parameters  $x_{w_o}$ ,  $y_{w_o}$  and  $a_w$ ,  $b_w$ . In the previous work by Kubota et al.,<sup>4</sup> which assumed that the entire wall was flexible, this integral over the flexible area  $A_f$  divided by  $A_f$  evaluated simply to  $1/4$ , which, in general, is not true here since in most cases only a portion of the wall is flexible.

### Numerical Study

#### Description

For the numerical study, a rectangular cavity was considered (Fig. 2). One of its walls, or a portion thereof, was assumed to vibrate in an infinite number of structural modes. The wall was driven with banded white noise. The effects of varying both the size and position of the vibrating portion of the wall were studied. The size of the wall varied from full wall (100% wall area) down to a point (0.004% wall area).

The quantities used in the study were ratios of mean square pressure predicted by CMA to that predicted by AMA. Initially, spatial averages using both CMA and AMA were taken in order to avoid introducing the response location within the cavity as an additional parameter. Later, the local acoustic pressure responses at corner points, edge points, points on the face, and points in the interior were considered for these cases.

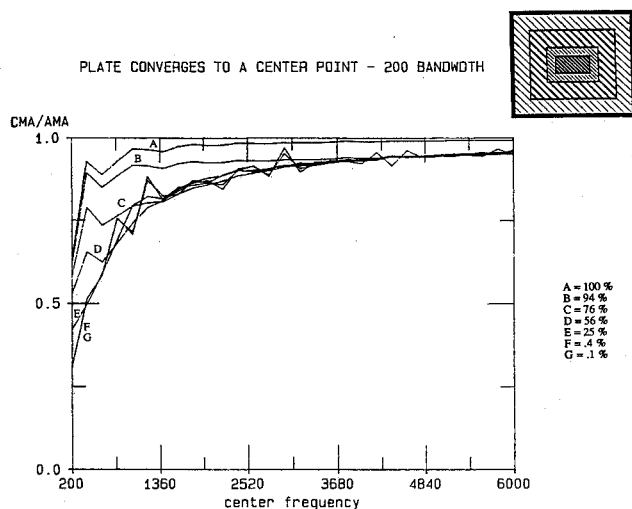


Fig. 3  $\langle \text{CMA} \rangle / \langle \text{AMA} \rangle$  vs center frequency, 200-Hz fixed bandwidth, flexible area shrinks to center.

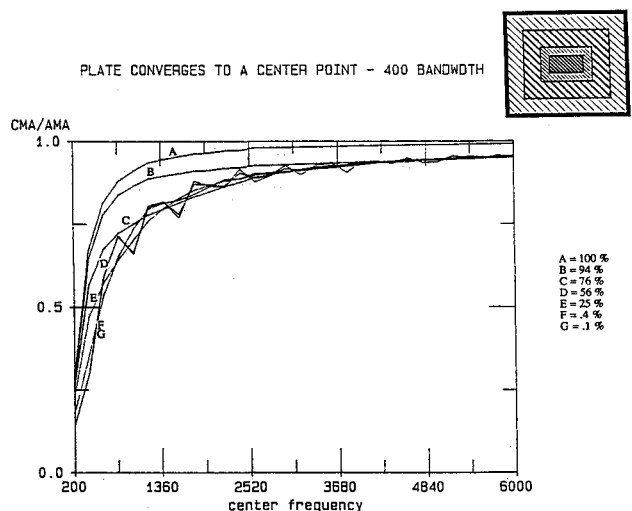


Fig. 4  $\langle \text{CMA} \rangle / \langle \text{AMA} \rangle$  vs center frequency, 400-Hz fixed bandwidth, flexible area shrinks to center.

## Results

### Spatially Averaged Case

The ratio of the spatial average of CMA to the spatial average of AMA [Eq. (4)] for the case where the oscillating portion of the wall converges to a center point is shown in Figs. 3-5. Each figure shows the spatially averaged CMA to spatially averaged AMA ratio for a different frequency bandwidth (200, 400, and 600 Hz) as a function of center frequency. The bandwidth  $\Delta\omega$  is defined as  $\Delta\omega = \omega_{\max} - \omega_{\min}$ , and the center frequency  $\omega_c$  as  $\omega_c^2 = (\omega_{\max} \cdot \omega_{\min})$ , where  $\omega_{\max}$  and  $\omega_{\min}$  are the maximum and minimum frequencies of the frequency interval. All acoustic modes are assumed to have the same modal critical damping ratio  $\zeta$  ( $\zeta \ll 1$ ).

As can be seen from Figs. 3-5, all results approach unity as the center frequency becomes large. The larger bandwidths yield smoother curves, and the smaller bandwidths approach the asymptote slightly more rapidly. Kubota et al.<sup>4</sup> found similar trends regarding bandwidth effects in the related work. However, what was not expected was that departure from the entire wall oscillating caused little change in the spatially averaged CMA/AMA ratio for the cavity. This was most likely due to the fact that the oscillating plate was centered about the midpoint on the wall and that all modes are symmetric or antisymmetric about that point.

In Fig. 6, the result of the spatially averaged CMA/AMA ratio [Eq. (4)] for the oscillating plate of variable area and convergence to a point in the corner are shown. Again, plots that correspond to different frequency bandwidths yield similar results, and so only the 400-Hz fixed bandwidth plot is shown. In this case, there is a family of curves that approaches unity as center frequency (and therefore, number of modes) increases, as expected. However, the asymptote is approached from above rather than below for all plates smaller than the quarter wall. The quarter-wall case is equivalent, in terms of the CMA/AMA ratio, to the full wall due to symmetry. The cases where the plate is larger than a quarter panel approach from below as did the center point cases. For those cases in which the vibrating wall is smaller than a quarter panel, not only does the curve approach the asymptote from above, but as the oscillating portion of the wall better approximates a point, the peak of the curve approaches 4 and is slower to drop off to the asymptotic limit of 1. This region of elevated sound pressure level is similar to the intensification zones for structural systems discussed in Crandall,<sup>6</sup> Itao and Crandall,<sup>7</sup> and Crandall and Kulvets<sup>8</sup> and for structural-acoustic systems in Kubota et al.<sup>4</sup> However, the intensification is due to excitation location rather than response location.

It may first appear as if the AMA result does not account for this intensification. However, it was assumed that the excita-

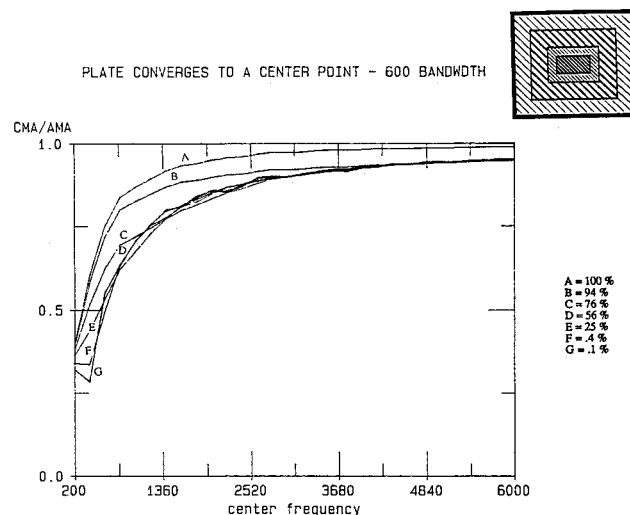


Fig. 5  $\langle \text{CMA} \rangle / \langle \text{AMA} \rangle$  vs center frequency, 600-Hz fixed bandwidth, flexible area shrinks to center.

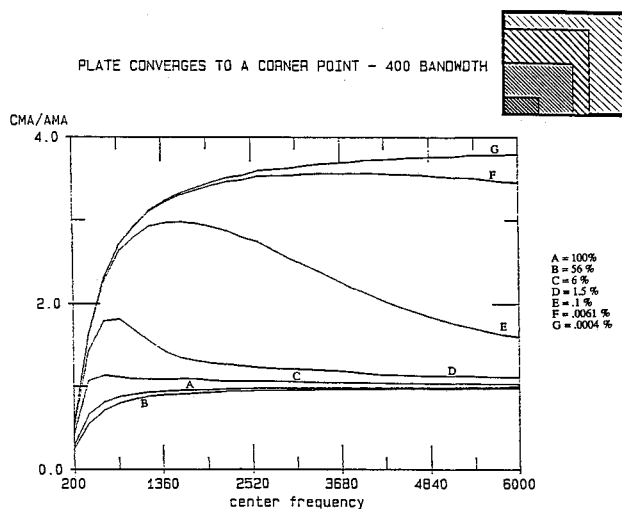


Fig. 6  $\langle \text{CMA} \rangle / \langle \text{AMA} \rangle$  vs center frequency, 400-Hz fixed bandwidth, flexible area shrinks to corner.

Four Particular Points of Interest - denoted by A, B, C, D

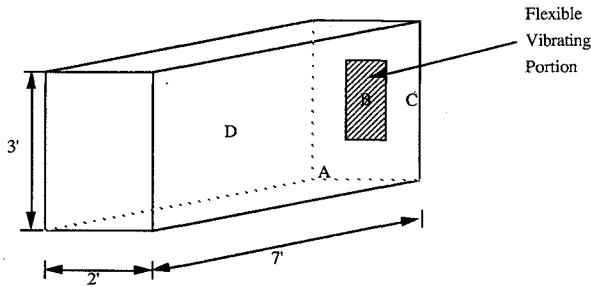
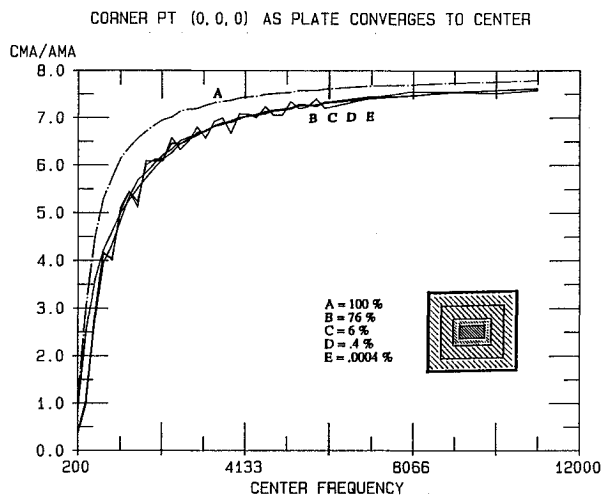
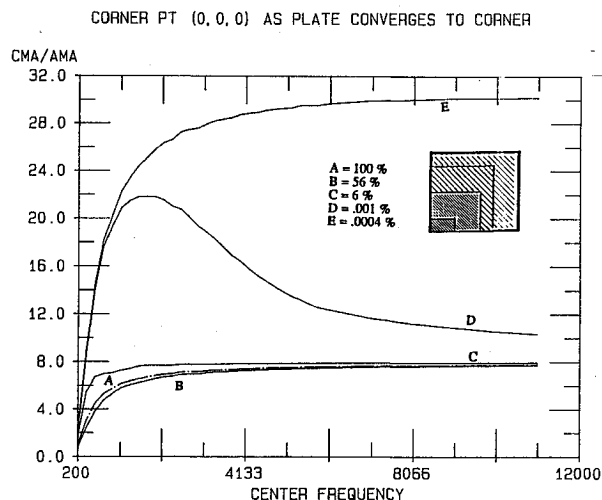


Fig. 7 Points at which the local response was predicted.

Fig. 8a Local CMA to  $\langle \text{AMA} \rangle$  ratio vs center frequency for point A, flexible area shrinks to center.Fig. 8b Local CMA to  $\langle \text{AMA} \rangle$  ratio vs center frequency for point A, flexible area shrinks to corner.

tion occurs away from a corner or an edge of the wall in computing the integral over the flexible area in the AMA expression. The effect of excitation intensification can be included in the AMA expression and, for corner excitation, would provide a factor of 4 increase. In addition to studying the effects of varying size and position of the oscillating portion of the wall in a spatially averaged sense, the local response was also calculated.

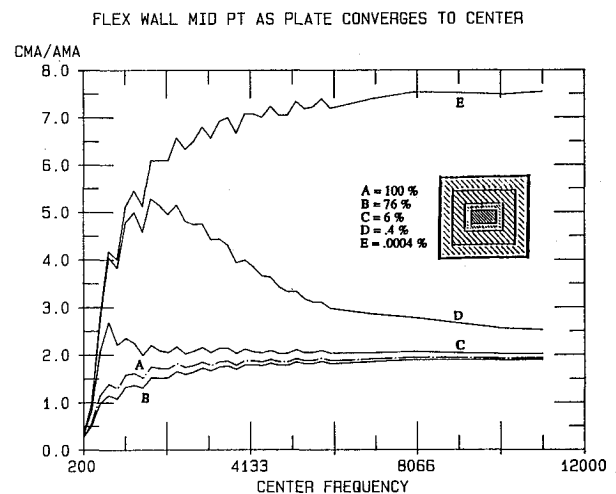
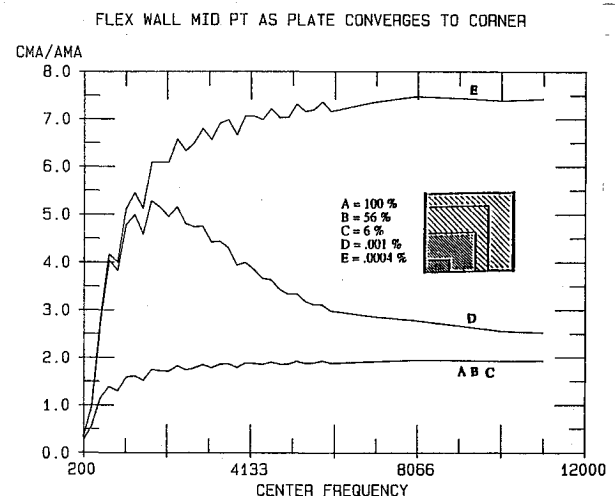
#### Local Response

The effect of position in the cavity was determined by considering the local response. This was again done for both con-

vergence of the vibrating plate from a full vibrating wall down to a vibrating point in the center and convergence to a point in a corner of the wall. The results are presented as a ratio of the mean square pressure evaluated at particular points in the cavity using CMA to the spatially averaged mean square pressure predicted by AMA. This ratio was computed for many center frequencies at a constant bandwidth of 400 Hz. There was no need to vary the bandwidth since Figs. 3-5 show little variation with bandwidth. The result was computed for various center frequencies in 200-Hz bandwidth increments up to a center frequency of 6000 Hz. Beyond 6000 Hz, 1000-Hz bandwidth increments were taken up to 11,000 Hz. This produces a smoother looking curve beyond 6000 Hz due to the larger frequency bandwidth increments.

Initially, four special response points were considered (see Fig. 7): the corner point (0,0,0), the midpoint of the flexible wall, the midpoint of the entire cavity, and a point on the wall along the centerline (1.8, 1.5, 0). For these four points, the ratio of CMA to spatially averaged AMA was plotted as a function of center frequency in Figs. 8-11.

Taking the corner point first (point A in Fig. 7), Fig. 8a shows that, as the plate converges to the center of the wall, the response of the corner approaches a pseudoasymptote of 8, whereas for convergence of the plate to the corner (Fig. 8b), this same point has a pseudoasymptote of 32, a factor of 4 greater. The idea of a pseudoasymptote will be discussed in the following section. The factor of 4 comes from the excitation

Fig. 9a Local CMA to  $\langle \text{AMA} \rangle$  ratio vs center frequency for point B, flexible area shrinks to center.Fig. 9b Local CMA to  $\langle \text{AMA} \rangle$  ratio vs center frequency for point B, flexible area shrinks to corner.

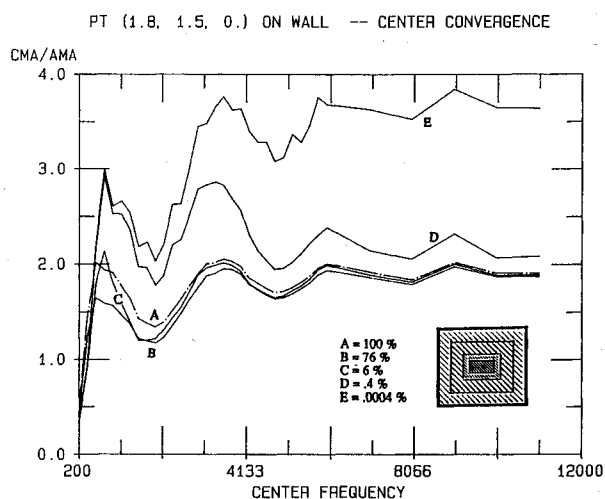


Fig. 10 Local CMA to  $\langle \text{AMA} \rangle$  ratio vs center frequency for point C, flexible area shrinks to center.

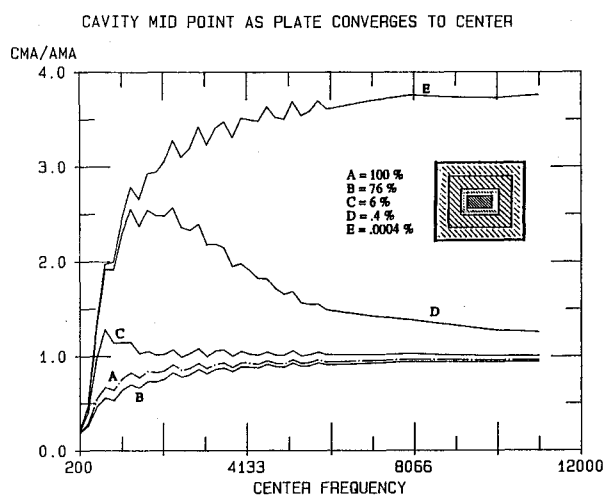


Fig. 11 Local CMA to  $\langle \text{AMA} \rangle$  ratio vs center frequency for point D, flexible area shrinks to center.

location (i.e., the location of the point source rather than the point of evaluation being in the corner), as was seen in the spatially averaged cases. Recall that when a point source was in the corner the spatial average was 4 times greater than when the point source was in the center of the wall.

Figures 9a and 9b show that, at the midpoint of the flexible wall (point B in Fig. 7), both types of convergence yield a pseudoasymptote of 8. Since this point is on the wall, its expected pseudoasymptote is 2. However, when the excitation is in the corner (Fig. 9b), this is increased by a factor of 4, hence the value 8. Five curves are actually plotted; only the curves representing the smallest plate areas (0.01 and 0.004%) deviate significantly from the others. On the other hand, when the excitation location and the response location are at the center of the wall (Fig. 9a), the response there is also increased by a factor of 4. This phenomenon is similar to the intensification observed by Kubota and Dowell<sup>3</sup> in experiments where point loads are applied to a rectangular plate. They found that, in the limit of a large number of responding modes on the plate, the response of the plate as measured by the plate acceleration at various places on the plate surface was nearly uniform. The accelerations were significantly higher near the application points of the point loads. Because of symmetry, the effect of

a point sound source acting at the center of the wall is to divide the rectangular cavity into quadrants (defined by cutting perpendicular planes through the point source). In the newly defined subcavities, this point where the source is located is now a corner point. The response at a corner point is eight times greater than the interior region, and so the pseudoasymptote of 8 is appropriate for this case.

Kubota and Dowell<sup>3</sup> also found hot lines running perpendicularly through the point force. To test for these in this acoustic cavity analysis, a point along one of the anticipated hot plates was studied (point C in Fig. 7). Since this point is on the face, it is expected to have a pseudoasymptote of 2.0, which is indeed the case if the full wall is moving (dotted line in Fig. 10). However, in the case of center convergence (i.e., analogous to a point load acting at the center of the structural wall), this point lies on a hot plane, and Fig. 10 shows a pseudoasymptote of 4. Assuming that the hot planes divide the cavity into subcavities, this point is on an edge of a subcavity. Therefore, the value of 4 is appropriate since the response at an edge is four times greater than the interior. When the oscillating portion of the wall converges to the corner, the pseudoasymptote is 8. This is consistent with previous findings for

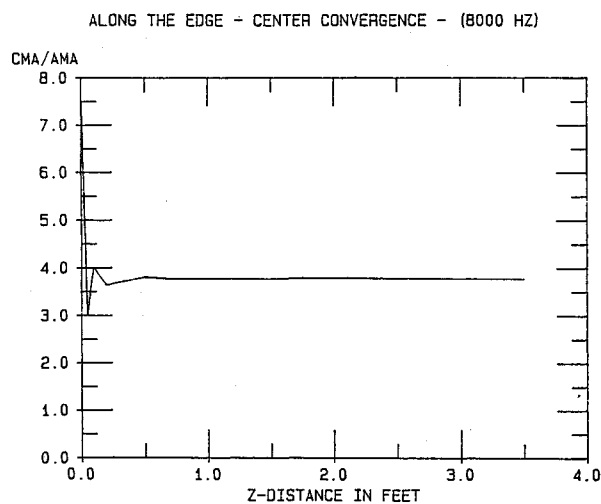


Fig. 12 Local CMA to  $\langle \text{AMA} \rangle$  ratio vs distance along an edge of the cavity away from a corner, with a point sound source in the center of the wall.

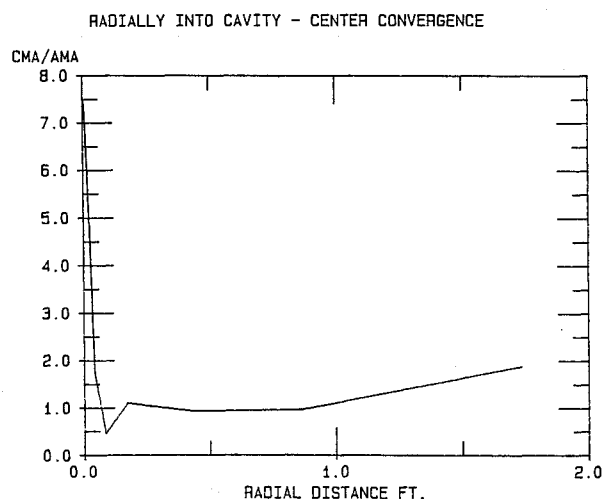


Fig. 13 Local CMA to  $\langle \text{AMA} \rangle$  ratio vs distance radially into the cavity away from a corner, with a point sound source in the center of the wall.

corner convergence since it represents a factor of 4 increase over the expected value for a point on a wall.

Response at the midpoint of the entire cavity (point D in Fig. 7) was also considered. At an interior point such as this, the expected asymptote is 1.0. However, when the plate converges to the center of the wall (Fig. 11), this point lies on a plane of symmetry resulting in a factor of 4 increase. Similar to the previous case, this point now lies on an edge of a newly defined subcavity. The edge point response is four times greater than the interior, and so the center convergence case is consistent. When the plate converges to a corner of the wall, again a fourfold increase is expected, due to the previous results for the spatially averaged cases, and the result is a pseudoasymptote of 4 (see curve E in Fig. 11).

Points A–D were studied as the plate size was allowed to vary, for the two cases (sound source shrinking from a full wall to a point sound source in a corner of the wall, and to a point in the center of the wall) as a function of center frequency (for a fixed bandwidth). Next, the plate size was fixed at 0.004% of the wall area, corresponding to a vibrating point. The center frequency was fixed at a value at which the pseudoasymptotes had previously been reached (8000 Hz), and the bandwidth was fixed at 400 Hz. The distance into the cavity from the vibrating wall was varied. Sample plots of local CMA to spatially averaged AMA vs distance into the cavity are shown in Figs. 12 and 13.

In Fig. 12, the sound source (vibrating point) is located in the center of the wall, and the response is plotted along an edge. The peak response in the corner is 8. Moving away from the corner, the response then oscillates before approaching the asymptote for an edge, which is 4.0. The data are symmetric in the  $z$  direction, as can be shown analytically. Therefore, only half of the edge length is plotted (3.5 out of 7.0 ft). The purpose of this plot is to show that there is a region where the transition is made from the increased (intensification) value to the nearly uniform value farther away. Further studies are needed to examine this transition zone and the parameters that determine its thickness.

Figure 13 is a plot of the response in a radial direction away from the corner of the cavity for the sound source in the center of the wall. The radial direction is defined by the line  $x = y = z$ , and the radial distance is equal to the square root of  $(x^2 + y^2 + z^2)$ . Since the point source is in the center of the wall, hot lines exist that run down the center of the cavity. Because of these hot lines, which redefine new effective boundary points, the cavity interior is no longer uniform, as is shown in Fig. 13. After the radial distance of 1.0, the response begins to increase, and approaches a value of 2.0, as if there were a wall or face there. This is not a physical boundary created by the cavity geometry, but rather an artificial boundary created by the point source. If the same radial trajectory is taken with the point source located in the corner, the response of the interior is uniform. The peak value in the corner is 32; the response then oscillates and eventually approaches a uniform interior value of 4.0. This plot shows the theoretical existence of hot planes or surfaces inside the cavity that are created by a point source acting at the center of the wall.

In summary, for a vibrating point at the center of the wall, the asymptotic limit for points that do not lie on hot planes is 1.0 for interior points, 2.0 for points on a face, 4.0 for points on an edge, and 8.0 for corner points. Also, the corner convergence cases yield the same relationships between locations but the magnitudes are increased by a factor of 4. Hot planes can be thought of as dividing the cavity into subcavities or quadrants along lines of symmetry. Each subcavity then produces its own corner, edge, and face points, with the respective sound pressure levels relative to each other, thereby redefining effective boundary points. The intensification results that were obtained here were through the use of CMA; however, AMA is capable of predicting intensification as well, as is pointed out in the next section. In subsequent work,<sup>11</sup> intensification zones are studied using an extension of the AMA method.

## Discussion

The term in the CMA/AMA equation [Eq. (4) or (5)] that is affected by changing the flexible area size and location of the flexible portion is

$$\iint_{A_f} F_r^2(x, y, z_o) dx dy / A_f$$

This can be thought of as a spatial average of the acoustic modal function in two dimensions ( $x$  and  $y$ ). The expected result would be  $1/4$ , unless the argument of one or both cosine functions (in  $F_r$ ) is always zero or a multiple of  $\pi$ . When the plate converges to a point in the corner, the  $x$  and  $y$  values are essentially zero; therefore, the value for the cosine is equal to 1 and the spatial average would then be 1.0 rather than  $1/4$ . Mathematically, the effect of shrinking the area down to a point in the corner yields a fourfold increase in the relative mean square pressure locally or spatially averaged.

However, one can imagine driving the frequency up so high that the approximated corner point no longer behaves like a point compared to an acoustic wavelength. This occurs when the acoustic wavelength becomes so small that the fixed physical size of the sound source is much larger than the wavelength of sound at that frequency. It is for this reason that the term pseudoasymptote has been used rather than asymptote. As the center frequency becomes sufficiently large (i.e., wavelength sufficiently small), the true asymptote will always be 1.0 for the spatially averaged CMA/AMA ratio.

Throughout this study, the numerical results have been presented either as the ratio of spatially averaged CMA to spatially averaged AMA,  $\langle \text{CMA} \rangle / \langle \text{AMA} \rangle$ , or for the ratio of local CMA response to spatially averaged AMA response. Other possible ratios could have been used. An alternative choice could have been the ratio of local CMA to local AMA. However, this ratio would not show any variation between points on a boundary and points in the interior. It would approach 1.0 at high center frequencies for all points if the excitation were in the center, or 4.0 if the excitation were in the corner, as is shown in the following analysis.

The local AMA result is [Eq. (2)]

$$\frac{\bar{p}^2}{(\rho_o c_c^2)^2} \cong \frac{\pi A_f}{4 V^2} \Phi_w(\omega_c) \frac{A_f \Delta N^A \langle F_c^2 \rangle}{(M_c^A)^2 (\omega_c^A)^3 \zeta_c^A \langle Z_c^2 \rangle} \sum_r \frac{F_r^2(x, y, z)}{\Delta N^A}$$

whereas the spatially averaged AMA result (derived in Ref. 4) is

$$\frac{\langle \bar{p}^2 \rangle}{(\rho_o c_c^2)^2} \cong \frac{\pi \Delta N^A}{4 \Delta \omega^A} \left( \frac{A_f}{V} \right)^2 \frac{\Delta \omega \Phi_w(\omega_c)}{(\omega_c^A)^3 \zeta_c^A \langle Z_c^2 \rangle} \quad (6)$$

Therefore, the ratio of local AMA to spatially averaged AMA is

$$(\text{AMA})_{\text{local}} / \langle \text{AMA} \rangle_{\text{spatial average}} = \left[ \sum_r F_r^2(x, y, z) / \Delta N^A \right] / \langle F_c^2 \rangle$$

The numerator

$$\left[ \sum_r F_r^2(x, y, z) / \Delta N^A \right]$$

is equal to  $1/8$  when  $x$ ,  $y$ , and  $z$  are not zero or  $L_x$ ,  $L_y$ ,  $L_z$ . It is equal to  $1/4$  when one of the values of  $x$ ,  $y$ , or  $z$  is equal to 0 or the length of the cavity in the appropriate direction, which is true on any face. Similarly, the numerator becomes  $1/2$  for an edge point and 1 for a corner point.

The spatially averaged acoustic modal function evaluated at the center frequency  $\langle F_c^2 \rangle$ , which comprises the denominator of the  $(\text{AMA})_{\text{local}} / \langle \text{AMA} \rangle_{\text{spatial average}}$  ratio, is always equal to  $1/8$ . Therefore, the  $(\text{AMA})_{\text{local}} / \langle \text{AMA} \rangle_{\text{spatial average}}$  is summarized in Table 1.

**Table 1 Local to spatial average-AMA ratios**

Location	AMA <sub>local</sub> / (AMA)
Corner	(1)/(1/8) = 8
Edge	(1/2)/(1/8) = 4
Face	(1/4)/(1/8) = 2
Interior	(1/8)/(1/8) = 1

Recall that the local CMA to spatially averaged AMA ratio for the center convergence case yields pseudoasymptotes of 8 in the corner, 4 on an edge, 2 on a face, and 1 in the interior. These ratios are four times greater if the excitation is in a corner.

This indicates that, for a large number of modes, the AMA results agree locally with the exact (CMA) results predicted when the oscillating wall is a full wall or converging toward the center. For corner convergence, the difference is a factor of 4. In deriving the AMA result used in this study, it was assumed that the excitation occurs at a location other than in a corner or on an edge, which accounts for the factor of 4 difference between center excitation and corner excitation, as explained previously. It is possible to incorporate the excitation location effect into the AMA result, if desired.

### Conclusions

An AMA approach has been developed and applied to a coupled structural-acoustic problem. It is broadly applicable to any linear dynamic system at high frequency regardless of geometry, assuming that the damping is small. Further work is needed to develop an AMA result that is applicable for cases involving large damping.

It is an extremely flexible approach and can be developed in accord with the nature of the system under study through inclusion of a series of simplifying assumptions. This technique can thereby bridge the gap between CMA and SEA in terms of computational requirements and predictive capability. In that AMA is developed from CMA, it retains the capability to predict spatial variations (intensification) in sound pressure levels or other relevant responses, something of which SEA is not capable. On the other hand, simplifications arising from the nature of the forces and the number of structural and acoustic modes involved result in a process that does not require individual modal characteristics. This greatly reduces the number of calculations required relative to CMA.

A rectangular acoustic cavity, with five rigid walls, was chosen to investigate the capabilities of AMA. Spatial averages and local behavior for sound pressure levels were calculated for a number of cases involving the location and size of the sound source on the wall. For the spatially averaged cases, intensification due to source location was observed. In particular, when a point sound source was located in the corner as opposed to the center of a wall, the spatially averaged sound pressure ratio was increased by a factor of 4.

In addition to the spatial average, the local response was also calculated. The local response of the cavity interior is nearly uniform, with the exception of points on the structural boundary (walls, edges, and corners), when one entire wall of the rectangular cavity is vibrating. However, when only a portion of one wall vibrates, and particularly when this portion approaches a vibrating point, there are further exceptions. Perpendicular planes (hot planes) that run through the vibrating point were found to divide the cavity into subcavities, which have new corners, edges, and walls. New subcavity corners, edges, and walls exhibit the same relative increase as the original corners, edges and walls, which is eight, four, and two times greater than the interior, respectively.

### Acknowledgments

This work was supported by the Structural Acoustics Branch of NASA Langley Research Center through Grant NAG-1-709 and NASA Graduate Student Researchers Program Fellowship NGT-50342. The authors would like to thank Donald B. Bliss of Duke University for his insightful comments and discussions related to this work.

### References

- <sup>1</sup>Dowell, E. H., "Vibration Induced Noise in Aircraft: Asymptotic Modal Analysis and Statistical Energy Analysis of Dynamical Systems," United Technologies Research Center, R82-112447, 1983.
- <sup>2</sup>Dowell, E. H., and Kubota, Y., "Asymptotic Modal Analysis and Statistical Energy Analysis of Dynamical Systems," *Journal of Applied Mechanics*, Vol. 52, No. 4, 1985, pp. 949-957.
- <sup>3</sup>Kubota, Y., and Dowell, E. H., "Experimental Investigation of Asymptotic Modal Analysis for a Rectangular Plate," *Journal of Sound and Vibration*, Vol. 106, No. 2, 1986, pp. 203-216.
- <sup>4</sup>Kubota, Y., Dionne, H. D., and Dowell, E. H., "Asymptotic Modal Analysis and Statistical Energy Analysis of an Acoustic Cavity," *Journal of Vibration, Acoustics, Stress and Reliability in Design*, Vol. 110, No. 3, 1988, pp. 371-376.
- <sup>5</sup>Lyon, R. H., *Statistical Energy Analysis of Dynamical Systems: Theory and Applications*, MIT Press, Cambridge, MA, 1975.
- <sup>6</sup>Crandall, S. H., "Random Vibration of One- and Two-Dimensional Structures," *Developments in Statistics*, Vol. 2, edited by P. R. Krishnaiah, Academic, New York, 1979, pp. 1-82.
- <sup>7</sup>Itao, K., and Crandall, S. H., "Wide-Band Random Vibration of Circular Plates," *Journal of Mechanical Design*, Vol. 100, 1978, pp. 690-695.
- <sup>8</sup>Crandall, S. H., and Kulvets, A. P., "Source Correlation Effects on Structural Response," *Application of Statistics*, edited by P. R. Krishnaiah, North-Holland, New York, 1977, pp. 168-182.
- <sup>9</sup>Dowell, E. H., "Reverberation Time, Absorption, and Impedance," *Journal of the Acoustical Society of America*, Vol. 64, No. 1, 1978, pp. 181-191.
- <sup>10</sup>Dowell, E. H., Gorman, G. F., III, and Smith, D. A., "Acoustoelasticity: General Theory, Acoustic Natural Modes and Forced Response to Sinusoidal Excitation, Including Comparisons with Experiment," *Journal of Sound and Vibration*, Vol. 52, No. 4, 1977, pp. 519-542.
- <sup>11</sup>Peretti, L. F., and Dowell, E. H., "Study of Intensification Zones in a Rectangular Acoustic Cavity," *AIAA Journal*, Vol. 30, No. 5, pp. 1199-1206.